Hiremath, L. S., Hiremath, S. T., Rychlik, W., Joshi, S., Domier, L. L., & Rhoads, R. E. (1989) *J. Biol. Chem. 264*, 1132.
Johnson, R. A., & Walseth, T. F. (1979) in *Advances in Cyclic Nucleotide Research* (Brooker, G., Greengard, P., & Robison, G. A., Eds.) Vol. 10, p 135, Raven Press, New York.
Knorre, D. G., Kurbatov, V. A., & Samukov, V. V. (1976) *FEBS Lett. 70*, 105.
Kometani, T., Watt, D. S., Ji, T., & Fitz, T. (1985) *J. Org. Chem. 50*, 5384.
Laemmli, U. K., & Favre, M. (1973) *J. Mol. Biol. 80*, 575.
Levya, E., Platz, M. S., Persey, G., & Wirz, J. (1986) *J. Am. Chem. Soc. 108*, 3783.
Markwell, M. A. K., & Fox, C. F. (1978) *Biochemistry 17*, 4807.
McCubbin, W. D., Edery, I., Altmann, M., Sonenberg, N., & Kay, C. M. (1988) *J. Biol. Chem. 263*, 17663.
McCubbin, W. D., Edery, I., Altmann, M., Sonenberg, N., & Kay, C. M. (1989) *FEBS Lett. 245*, 261.
Ofengand, J., & Henes, C. (1969) *J. Biol. Chem. 244*, 6241.
Patzelt, E., Blaas, D., & Kuechler, E. (1983) *Nucleic Acids Res. 11*, 5821.
Pelletier, J., & Sonenberg, N. (1985) *Mol. Cell. Biol. 5*, 3222.
Ray, B. K., Lawson, T. G., Kramer, J. C., Cladaras, M. H., Grifo, J. A., Abramson, R. D., Merrick, W. C., & Thach, R. E. (1985) *J. Biol. Chem. 260*, 7651.
Rhoads, R. E. (1988) *Trends Biochem. Sci. 13*, 52.
Rychlik, W., Gardner, P. R., Vanaman, T. C., & Rhoads, R. E. (1986) *J. Biol. Chem. 261*, 71.
Rychlik, W., Domier, L. L., Gardner, P. R., Hellmann, G. M., & Rhoads, R. E. (1987a) *Proc. Natl. Acad. Sci. U.S.A. 84*, 945.
Rychlik, W., Russ, M. A., & Rhoads, R. E. (1987b) *J. Biol. Chem. 262*, 10434.
Shields, C. J., Chrisope, D. R., Schuster, G. B., Dixon, A. J., Poliakoff, M., & Turner, J. J. (1987) *J. Am. Chem. Soc. 109*, 4723.
Smith, P. A. S., Hall, J. H., & Kan, R. O. (1962) *J. Am. Chem. Soc. 84*, 485.
Sonenberg, N. (1981) *Nucleic Acids Res. 9*, 1643.
Sonenberg, N. (1988) *Prog. Nucleic Acid Res. Mol. Biol. 35*, 173.
Sonenberg, N., & Shatkin, A. J. (1977) *Proc. Natl. Acad. Sci. U.S.A. 74*, 4288.
Sonenberg, N., Rupprecht, K. M., Hecht, S. M., & Shatkin, A. J. (1979) *Proc. Natl. Acad. Sci. U.S.A. 76*, 4345.
Tahara, S. M., Morgan, M. A., & Shatkin, A. J. (1981) *J. Biol. Chem. 256*, 7691.
Webb, N. R., Chari, R. V. J., DePillis, G., Kozarich, J. W., & Rhoads, R. E. (1984) *Biochemistry 23*, 177.

Conformation of Methyl β-Lactoside Bound to the Ricin B-Chain: Interpretation of Transferred Nuclear Overhauser Effects Facilitated by Spin Simulation and Selective Deuteration†

V. L. Bevilacqua, D. S. Thomson,‡ and J. H. Prestegard*
Department of Chemistry, Yale University, New Haven, Connecticut 06511
Received November 28, 1989; Revised Manuscript Received February 16, 1990

ABSTRACT: Spin simulation and selective deuteration have been used to aid in the interpretation of 1D transferred nuclear Overhauser effect (TRNOE) NMR experiments on ricin B-chain/ligand systems. Application of these methods has revealed a change in the conformation of deuterated methyl β-lactoside upon binding to the ricin B-chain which results in a slight change in glycosidic torsional angles which appear to dominate in the solution conformation. The combination of simulation and experiment also shows an important sensitivity of TRNOE magnitudes to dissociation rate constants and available spin-diffusion pathways for the ricin B-chain/ligand systems under study. The sensitivity to dissociation rates allows determination of rate constants for methyl β-lactoside and methyl β-galactoside of 50 and 300 s^{-1}, respectively.

Cell membranes must interact with their external environment as a part of important biological processes such as cell recognition, intercellular adhesion, and growth regulation. Moreover, a number of pathological events begin with a recognition step at the cell membrane. Specific peptides and proteins, including hormones, antibodies, viral coat proteins, bacterial toxins, and lectins, frequently mediate interactions with the cell. Thus, one step toward understanding the interactions of a cell with its environment begins with understanding these mediator molecules and their interaction with membranes.

Ricin, a toxic lectin of MW 65 000 found in castor bean seeds, shares a general subunit composition and membrane interaction mode with several other toxic lectins and agglutinins (Olsnes & Pihl, 1982). Especially notable is its relation to *Ricinus communis* agglutinin, a larger lectin known to mediate intermembrane contact and thereby specifically enhance Ca^{2+}-induced fusion of certain membranes (Sundler & Wijkander, 1983). Ricin contains two subunits, the A- and B-chains (Ra and Rb,[1] respectively), covalently linked by a disulfide bond. The A-chain (MW 31 000) inhibits protein synthesis by inactivating the 60S ribosomal subunit. The

† This work was supported by U.S. Public Health Service Grant GM19035.
* Author to whom correspondence should be addressed.
‡ Present address: Cytel Corp., 11094 N. Torrey Pines Rd., La Jolla, CA 92037.

[1] Abbreviations: NOE, nuclear Overhauser effect; Rb, ricin B-chain; FID, free induction decay; 2D NOESY, two-dimensional NOE spectroscopy; SIR, selective inversion recovery; ISPA, independent spin pair approximation.

0006-2960/90/0429-5529$02.50/0

B-chain (MW 34000) binds to cell surface galactose moieties and mediates transport of the toxic subunit across the cell membrane (Houston & Dooley, 1982). In this respect, the Rb/cell interactions resemble a number of hormone/cell interactions and viral or bacterial infection mechanisms.

The amino acid sequence for Rb has been determined (Araki & Funatsu, 1985), and a crystal structure at 2.8 Å has been solved (Montfort et al., 1987). From this research and various binding studies, Rb appears to contain two β-galactose-specific noncooperative binding sites with slightly different affinities (Rutenber et al., 1987; Houston & Dooley, 1982; Yamasaki et al., 1985; Hatakeyama et al., 1987). The two binding sites involve similar amino acids, and the two binding domains appear to have resulted from an ancient gene duplication (Rutenber et al., 1987). However, the details of bound-ligand/binding-site interaction and conformation remain unknown.

NMR has become a popular method for obtaining detailed information about solution conformations of both small and large molecules of biological interest. However, many proteins (like Rb) are too large and/or insufficiently soluble for a total structure determination to be approached directly. Even in the study of bound ligands, broad resonances and interference from protein signals complicate analysis. In these cases, the transferred nuclear overhauser effect (TRNOE) provides an indirect approach to the determination of bound-ligand conformation (Clore & Gronenborn, 1982).

TRNOE takes advantage of chemical exchange to transfer bound-state information to the free state. Briefly, TRNOE involves measurement of negative NOEs on the free or averaged resonances of one ligand spin following irradiation of the free, bound, or averaged resonances of another ligand spin. This information transfer allows observation of effects developed in the bound state at a resonance from an abundant species with diminished effects from line broadening and protein interference.

The success of the TRNOE experiment is easily verified for exchanging systems by the observation that NOEs which are normally positive for small molecules become negative when relaxation in the bound state dominates. However, interpretation of these TRNOEs in terms of interproton distances in the complex often presents difficulties. Spin diffusion, which becomes efficient in large molecular weight systems, leads to a number of indirect transfers. Furthermore, in the case of intermediate-sized proteins, such as Rb, contributions from free-state ligand relaxation can further alter observed NOE intensities. Our strategy combines the selective inversion recovery (SIR) TRNOE time course experiment with a rigorous theoretical simulation and exploits selective deuteration of the ligand to simplify major indirect transfer pathways. We will focus on possible changes in conformation about the glycosidic bond for methyl β-lactoside (methyl 4-*O*-β-D-galactopyranosyl-β-D-glucopyranoside) upon binding to Rb and on the observed sensitivity of TRNOE time courses to ligand exchange rates.

Experimental Procedures

Materials. Ricin B-chain was purchased in phosphate-buffered saline solution from Sigma Chemical Co., St. Louis, MO. Lactose and methyl β-galactoside were also Sigma products.

The fully protonated methyl β-lactoside used in the experiments was prepared by the method of Smith and Van Cleve (1952). Briefly, 100 g of lactose was converted to the octaacetate. The octaacetate (10.0 g) was converted to acetobromolactose by the method of Fischer (1910), and 3.8 g of the acetobromolactose (not recrystallized, but pure as shown by NMR) was dissolved in 75 mL of MeOH (absolute). A total of 1.32 g of Ag_2CO_3 was added and the solution stirred in the dark for 19 h. Dry Norit charcoal was added, and the solution was filtered after 0.5 h. The solution was rotovapped to dryness, leaving white crystals. The crystals were dissolved in 58 mL of MeOH (absolute), and small pieces of Na metal were added until white crystals began to appear floating in solution. Although the reaction appeared to be complete in about 1 h, the solution was left at room temperature overnight. The crystals were filtered and washed with cold MeOH. ^{1}H NMR showed only methyl β-lactoside to be present.

The methyl β-lactoside used as a precursor for the deuterated form was synthesized by the method of Paulsen et al. (1985). To accomplish deuteration, we employed a Raney nickel catalyzed exchange reaction along the lines originally described by Koch and Stuart (1978). Raney nickel purchased as a slurry from Aldrich (Milwaukee, WI) was preexchanged in 99.7% deuterium oxide (MSD Isotopes, St. Louis, MO). Approximately 0.5 mL (settled volume) was added to 15 mg of methyl β-lactoside; 7 mL of D_2O was added. The mixture was refluxed under nitrogen for 15 min. At reaction termination the mixture was centrifuged, filtered through glass fiber, and passed through Chelex ion-exchange resin to remove remaining nickel impurities. To ease assignment of deuterated positions, the deuterated methyl β-lactoside was converted to the acetate (Ac_2O/py). The deuterated positions were determined by loss of signals in the previously assigned ^{1}H NMR spectrum.

Sample Preparation. All NMR samples were in D_2O at pH 6.5 (not corrected for isotope effects), 10 mM PO_4, 0.15 mM NaCl, and 0.02% NaN_3. For the sugar samples, concentrated aqueous solutions were made. Aliquots of the concentrated solutions were added to buffer and then lyophilized and exchanged twice with D_2O. The final samples were dissolved in D_2O.

Rb samples were concentrated and exchanged with deuterated buffer in Centricon-10 microconcentrators (Amicon, Danvers, MA). The Sigma solution containing the desired amount of Rb was concentrated to 0.04 mL. A total of 0.5–2.40 mL of D_2O buffer (99.8% D) was then added and the resulting solution concentrated again to 0.04 mL. This process was repeated two to four times. For all except the deuterated methyl β-lactoside sample, sugar was present at the desired final concentration throughout the exchange procedure. For the deuterated methyl β-lactoside sample, only the last exchange contained sugar.

The final solution in each case was transferred to an NMR tube and brought to 0.40 mL with deuterated buffer (99.96% D) containing ligand at the desired concentration. The final Rb concentration was measured with UV by use of an extinction coefficient ($E^{1\%}_{280nm}$,1cm) of 14.9 (Olsnes et al., 1975).

The methyl β-galactoside and fully protonated methyl β-lactoside samples were purged with N_2 gas for 10 min. All samples were used immediately after preparation or stored desiccated under N_2 at 4 °C.

NMR Procedures. ^{1}H NMR spectra were acquired at 30 °C with quadrature detection on a Bruker WM-500 or on a home-built spectrometer operating at 11.5 T (490-MHz proton frequency). 1D selective inversion recovery NOE experiments were carried out with the pulse sequence $\{D_1-180°(\text{selective})-T_m-90°-AQ\}_n$. The 1D saturation transfer NOE control (see Results and Discussion) was carried out with the pulse sequence $\{D_1-T_m(\text{saturate})-90°-AQ\}_n$. Here, D_1 is a relaxation delay, T_m is the mixing time, AQ is acquisition, and 180° or

90° represents magnetization rotation with rf pulses. Two FIDs were collected for all 1D NOE experiments, an NOE FID in which the decoupler was placed on the frequency of interest and a reference FID in which the decoupler was placed downfield of the protein resonances (about 3000 Hz from the on-resonance frequency). The two data sets were recorded by interleaving eight scans for the NOE FID with eight scans for the reference FID until a good signal to noise ratio in the difference spectrum between the two Fourier transformed sets was reached.

Quantitative analysis of macromolecular structures first requires an accurate integration of peak intensities. A well-resolved anomeric peak in the reference spectrum for each mixing time was integrated with standard processing software and set equal to one proton. Single proton peaks were integrated in the difference spectra and the NOEs recorded as a percent of the area of one proton. In cases where peaks overlapped extensively, a curve-fitting routine was used (SpectraCalc, Galactic Industries Corp., Salem, NH) to obtain the areas.

2D NOESY spectra (Jeener et al., 1979; Kumar et al., 1980; Wider et al., 1984) were acquired in the phase-sensitive mode by the States method (States et al., 1982). All data were transferred to a VAX 11/750 computer equipped with a CSPI Minimap array processor or to a VAXSTATION 3200 for processing.

Simulations. Simulations of 1D selective inversion experiments were carried out with a modification of a 2D NOESY simulation program written by Scarsdale (1989). Chemical exchange was included by modification of the Bloch equations as described in the literature by Clore and Gronenborn (1982).

Briefly, exchange is included for each free ligand spin *if* and for each bound spin *ib* in the following way:

$$dM_{if}/dt = (\rho_{if} + \rho_f^*)(M_{if} - M_{if0}) + \sum\sigma_{if,jf}(M_{jf} - M_{jf0}) + k_{-1}M_{ib} - k_1'M_{if}$$

$$dM_{ib}/dt = (\rho_{ib} + \rho_b^*)(M_{ib} - M_{ib0}) + \sum\sigma_{ib,jb}(M_{jb} - M_{jb0}) - k_{-1}M_{ib} + k_1'M_{if}$$

Here M_{ib} and M_{if} are the z components of the magnetization for the *if* and *ib* spins of the ligand molecule at any time t, M_{if0} and M_{ib0} are the equilibrium magnetizations of the free and bound states for these spins, ρ_{if} and ρ_{ib} are the total intramolecular spin–lattice relaxation rates of *if* and *ib* due to defined pairwise dipolar interactions within a ligand molecule, $\sigma_{if,jf}$ and $\sigma_{ib,jb}$ are the cross-relaxations between the ith and jth nuclei in the free and bound states, respectively, and ρ_f^* and ρ_b^* are terms added to account for relaxation effects not specifically associated with spin pairs within a single ligand molecule. Exchange is described by the rate constants k_1' and k_{-1}. These constants are reciprocal lifetimes for molecules in bound and free states. The forward rate is explicitly dependent on the free protein concentration; $k_1' = k_1[P]$. Free protein is in turn related to an equilibrium constant, $K_a = k_1/k_{-1}$, and a free ligand concentration taken to be approximately the total ligand concentration in our experiments.

Results and Discussion

β-Lactose in the crystalline form (Hirotsu & Shimada, 1974) exists in the structure depicted in Figure 1. Sugar rings are widely regarded as being predominantly in the chair form, so the glycosidic torsional angles ϕ and ψ and the exocyclic torsions which move the C_6 methylene group describe major conformational variations. It is clear that distance information relating the anomeric proton of galactose, H_1', to trans-

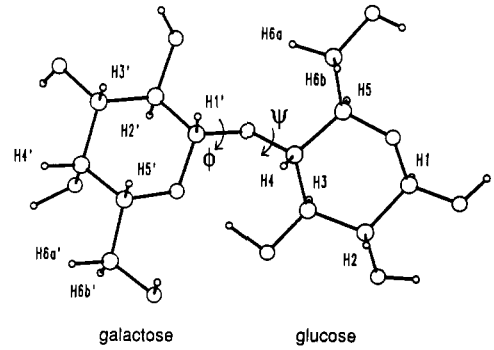

FIGURE 1: Crystal structure of methyl β-lactoside.

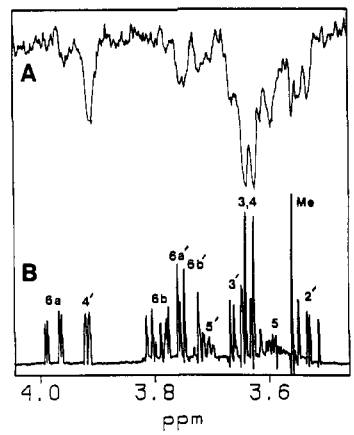

FIGURE 2: (A) 500-MHz ^{1}H 1D SIR TRNOE difference spectrum of methyl β-lactoside in the presence of ricin B-chain (T_m = 0.4 s). FIDs resulting from 1000 scans were zero filled from 16K to 32K, and a line broadening of 1.00 was applied before transformation. (B) 490-MHz ^{1}H NMR methyl β-lactoside spectrum. A Gaussian multiplication with Gaussian broadening of 0.15 and line broadening of −1.30 were applied before transformation.

glycosidic glucose protons H_4, H_5, and H_3 would be of major interest. The H_4 proton in the crystal structure, at 2.42 Å from H_1', would be expected to give strong NOEs, along with intraring protons H_3' and H_5' at 2.39 and 2.31 Å, respectively. Some weak contacts with H_5 or H_3 across the glycosidic bond might be expected and would be particularly useful in quantitation of conformational preference. The strong distance dependence of the NOE ($1/r^6$) should make NOEs to more remote protons virtually unobservable.

Figure 2 shows the data from a 1D SIR TRNOE experiment on methyl β-lactoside in the presence of Rb (sugar:protein = 22:1) in which the H_1' resonance (4.43 ppm) was inverted and the mixing time, T_m, was set to 0.4 s (Figure 2A). A one-dimensional spectrum of methyl β-lactoside with assignments is shown for comparison. Several features are worthy of note. First, it is clear from the negative difference peaks that the bound state dominates the NOEs when Rb is present. NOEs for small molecules in solution are positive for all one-step transfers of magnetization. Primary ^{1}H–^{1}H NOEs are negative only when effective correlation times for the species dominating the NOEs are larger than the reciprocal of the Larmor frequency. Peaks that can be associated with the expected H_1'–H_5', H_1'–H_3', and H_1'–H_4 transfers are easily observed and are strongly negative. Second, strong unexpected transfers occur. The extra peaks in the 3.60–3.65 ppm region could be explained on the basis of strong coupling between glucose protons 4 and 3, and possibly protons 4 and 5, leading to second-order effects. However, there are transfers to peaks assigned to remote protons on the galactose ring, particularly H_4', which cannot be explained in this way. If analyzed ac-

cording to an independent spin pair approximation (ISPA), intensities of resonances exhibit a $1/r^6$ relationship to other resonances in the difference spectra. The separation between H_1' and H_4' would therefore be comparable to that between H_1' and H_3' or H_1' and H_5'. Only if the ring adopted an energetically undesirable boat form for a significant fraction of time could the H_1'–H_4' transfer arise from a direct interaction. It is more probable that, with the relatively long mixing time for this spectrum (0.4 s), we are observing extensive secondary transfers, or spin diffusion.

A popular method of identifying secondary transfer is to look at the NOE buildup for time courses at mixing times less than 0.4 s. Secondary transfer curves should show an initial lag in buildup during this time. We examined spectra at 0.2- and 0.1-s mixing times and found similar relative levels of transfer to H_4'. Either spin diffusion is very efficient, or a rather unusual geometry exists. Since we were unable to obtain adequate signal to noise with a reasonable use of spectrometer time at mixing times less than 0.1 s, we decided to pursue this problem by comparing experimental results to spectral simulations which include the possibilities of secondary transfer.

In order to provide better quantitative data for a test of these simulation procedures, we first considered a simpler system, methyl β-galactoside. The geometry is less variable and the spectra are better resolved in the monosaccharide system than in the methyl β-lactoside disaccharide, while the galactose secondary transfer pathway of interest (from H_1 through H_5 and H_3 to H_4) remains.

1D SIR TRNOE experiments were carried out on two methyl β-galactoside/Rb samples at sugar:protein ratios of 10:1 and 41:1 and on the sugar alone for comparison. TRNOEs were negative for the Rb complexes, in contrast to the positive NOEs seen for the unassociated ligand. The H_5 and H_3 NOEs expected on the basis of the crystal structure geometry of methyl β-galactoside (Takagi & Jeffrey, 1978) appeared in both the unassociated and Rb-bound NOEs. Again, a large H_4 peak was seen in the Rb-bound case. This peak was absent in the unassociated experiment, as expected.

The simulation program employed goes a step beyond the independent spin pair approximation by allowing successive transfer of magnetization through the cross-relaxation rate constants, σ_{ij}. The program calculates ρ_i and σ_{ij} on the basis of an array of proton positions for a rigid molecular structure and an assumed isotropic tumbling of the whole molecule. These assumptions are not bad for the protein-bound state, and as long as relaxation effects in this state dominate the observation, free-state violations of the assumption have minimal consequences.

Simulations for the sugar alone were carried out with proton crystal structure coordinates (Takagi & Jeffrey, 1978) and with variations in the correlation time (τ_c) to fit the H_1 and H_5 experimental time course curves. Explicit treatment of protons on the *O*-methyl group was left out of the simulation since its rapid rotation reduces the magnitude of the interaction with remaining protons. Experiment supports this omission in that the NOE to the methyl peak is small. As shown in Figure 3, the experimental data for the remaining protons could be fit excellently with a τ_c of 6.5×10^{-11} s. No external relaxation (ρ^*) was necessary.

Simulations of data for methyl β-galactoside bound to Rb are, in principle, more difficult because many additional parameters can vary. ρ^* and τ_c factors for both bound and free species, plus rate constants for the exchange process, need to be included. However, the parameters pertaining exclusively

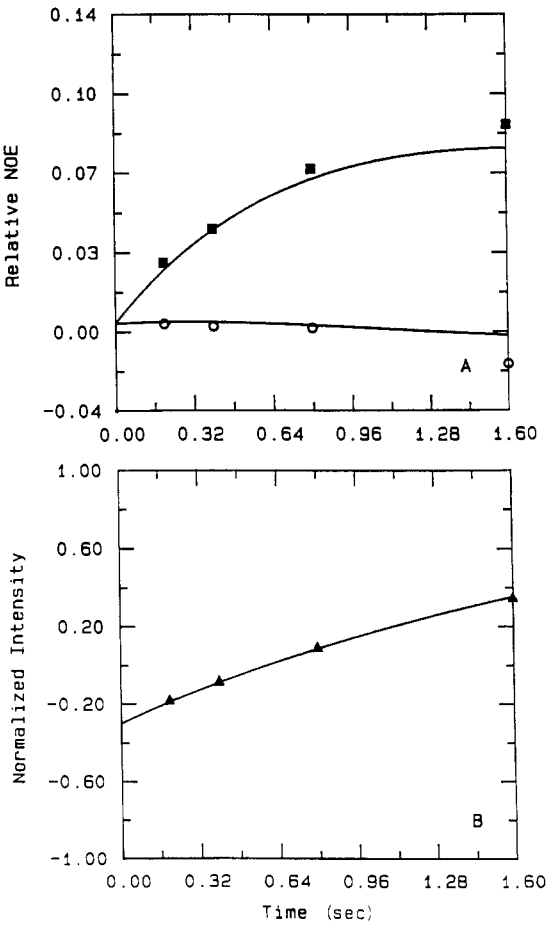

FIGURE 3: Experimental and simulated (—) curves for methyl β-galactoside. (A) H_5 (■) and H_4 (○) experimental results. Relative NOE is the intensity in the difference spectra as a fraction of the H_1 intensity in the reference spectra. (B) H_1 recovery (▲). Normalized intensity is the intensity in the irradiated spectra as a fraction of the H_1 intensity in the reference spectra.

to the free species can be taken from the fit described above, and known sample composition and ligand binding constants (K_a) can be used to eliminate one of the rate variables. Thus, with $\rho_f^* = 0\%$, $\tau_{cf} = 6.5 \times 10^{-11}$ s, and $K_a = 1.5 \times 10^4$ M^{-1} (Yamasaki et al., 1985), simulations were carried out for a range of k_{-1} values from 40 to 10^5 s^{-1} for both the 10:1 and 41:1 sugar to protein ratio data sets. At each k_{-1} value, ρ_b^* and τ_{cb} were varied to give an optimum fit to the H_1 and H_5 experimental data. At large k_{-1}, or very rapid exchange, the ratio of primary (H_5) to secondary (H_4) transfer in the simulations was larger than the ratio observed experimentally. As k_{-1} was decreased, the magnitudes of both primary and secondary transfer at the higher ratio decreased. However, the primary transfer magnitude decreased faster, lowering the primary to secondary transfer ratio. Figure 4 shows data from the experimental time courses and simulations with $k_{-1} = 10^2$ (solid lines) and $k_{-1} = 5.0 \times 10^2$ s^{-1} (dashed lines) for the samples prepared at 10:1 (A) and 41:1 (B) sugar to protein ratios. At $k_{-1} = 10^2$ s^{-1}, the H_5 simulation in both cases was within experimental error (solid squares), while the H_4 (open circles) fit was poor. At $k_{-1} = 5.0 \times 10^2$ s^{-1}, the H_4 simulation at both ratios was within experimental error, while the H_5 fit was worse, especially in (B). Optimum fit to both H_5 and H_4 experimental data was reached with a k_{-1} of 3.0×10^2 s^{-1}, a τ_{cb} of 4.3×10^{-8} s, and a ρ_b^* of 17%. ρ^* values are reported as a percentage of the relaxation rate of the inverted spin, H_1. The increase from 0% for free methyl β-galactoside to 17% for bound methyl β-galactoside is very likely due to contri-

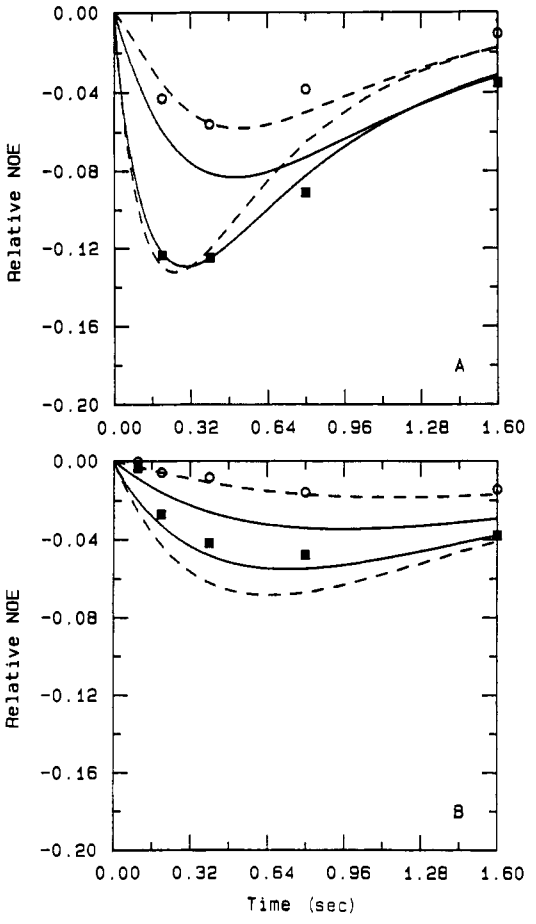

FIGURE 4: Experimental and simulated H_5 and H_4 curves for methyl β-galactoside in the presence of ricin B-chain. (■) H_5 and (○) H_4 experimental results. Simulations with k_{-1} = 100 (—) and 500 s^{-1} (– –), respectively. (A) Sugar:protein = 10:1; (B) sugar:protein = 41:1.

butions from cross relaxation between protons on galactose and protons on the protein.

The sensitivity of the TRNOE experiments to exchange rates, while generally recognized, is seldom appreciated. From the data described above, it is clear that extreme variation can occur when secondary transfer pathways are important. This variation can be rationalized in the limit of very slow exchange. As lifetimes in the bound state become long compared to cross-relaxation rates, molecules released to solution have had time to equilibrate magnetization among all coupled spins and TRNOEs to all sites become equal. Observations that H_4 NOEs can actually become larger than H_5 NOEs originate from selective cancellation of H_5-bound NOEs by the positive NOEs at this site that arise from molecules in solution.

Using a similar experiment/simulation procedure, we could, in theory, analyze the more structurally interesting methyl β-lactoside case. However, as previously discussed, the region of interest (H_4) is complicated by strong scalar coupling and spectral overlap. Thus, in order to reduce major diffusion pathways and simplify the spectrum, methyl β-lactoside was selectively deuterated. The results of the deuteration in terms of percent protonation remaining (observable ^1H signals) appear in Table I. Deuteration at H_4' eliminates spin diffusion through the H_1'–H_3'–H_4' and H_1'–H_5'–H_4' pathways and should greatly simplify interpretation of remaining NOEs. Partial elimination of the H_6', H_6, H_2', and H_2 protons should also help. Additionally, elimination of the H_3' and H_3 protons greatly simplifies the spectral region of interest, leaving H_5' and H_4 well resolved and easily integrable. Note the simplification in the H_4 region around 3.63 ppm shown in Figure 5C. Thus, the H_1'–H_5' transfer, important in calibrating transglycosidic distances in a disaccharide, is now easily quantitated, and H_1'–H_4 transfers are easily measurable.

Table I: Percent Remaining Protonation of Deuterated Methyl β-Lactoside

galactose ring		glucose ring	
position	% proton	position	% proton
H1′	100	H1	100
H2′	40	H2	33
H3′	0	H3	0
H4′	0	H4	100
H5′	100	H5	100
H6a′	50	H6a	75
H6b′	50	H6b	25
		OMe	100

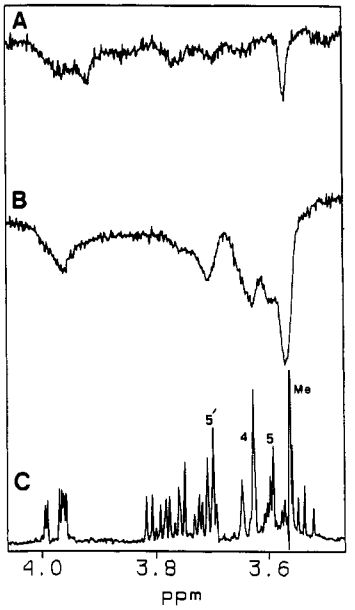

FIGURE 5: 490-MHz ^1H spectra. (A) Control TRNOE difference spectrum of methyl β-galactoside in the presence of ricin B-chain (T_m = 0.2 s; irradiation at 4.43 ppm). FIDs resulting from 2176 scans were zero filled from 16K to 32K, and a line broadening of 1.00 was applied before transformation. (B) TRNOE difference spectrum of deuterated methyl β-lactoside in the presence of ricin B-chain (sugar:protein = 6:1; irradiation on H_1' at 4.43 ppm; T_m = 0.2 s; size = 16K). (C) Deuterated methyl β-lactoside spectrum. A Gaussian multiplication with Gaussian broadening of 0.80 and line broadening of −1.50 were applied before transformation.

The results of a 1D SIR NOE experiment on the deuterated methyl β-lactoside/Rb sample appear in Figure 5B. As in the previous experiment, the TRNOEs are negative in contrast to the positive NOEs expected for an unassociated small molecule. Note the absence of the large H_1'–H_4' transfer in the TRNOE spectrum which occurred at 3.91 ppm in the fully protonated methyl β-lactoside experiment.

Among the NOEs seen, a peak assigned to the β-Me group is largest. This peak did not seem nearly so pronounced in the fully protonated sample. This transfer is most likely the result of the fact that selectivity for the H_1' (4.43 ppm) in this experiment was not achieved as well as in previous experiments. The glucose H_1 (4.39 ppm) peak was inverted to a larger extent than before, resulting in direct H_1–(β-Me) transfer. Also, several of the intense peaks in the fully protonated sample have been removed by deuterium substitution, so the β-Me group appears relatively larger than it would have in the fully protonated case.

Pronounced H_4 and H_5' peaks are observed as expected at 3.63 and 3.70 ppm. A transfer to H_5 of the glucose is also

observed at 3.58 ppm. While this could result in part from the partial inversion of the glucose H_1 proton, a 2D experiment, which has good frequency resolution of H_1 and H_1', shows some direct H_5 connectivity to H_1'. This could be an important piece of structural information. Also, note the apparent TRNOE at 3.97 ppm which could be interpreted as a large H_1'–H_{6a} transfer. Although there is a small H_1'–H_{6a} transfer seen in experiments on the sugar alone (to be presented later), the large size of the 3.97 ppm peak relative to the H_5' peak could indicate a shift in conformation toward smaller ϕ or ψ angles.

The H_5 and 3.97 ppm peaks mentioned above require an adequate control experiment. It is possible, for example, that the 3.97 ppm peak arises because of protein resonances which are selectively enhanced on inversion of other protein resonances underlying the H_1' resonance. A control experiment was therefore carried out with the methyl β-galactoside sample where the methyl β-galactoside to Rb ratio was 10:1. Methyl β-galactoside presumably occupies the same protein sites and induces similar protein conformation and chemical shift changes for Rb. However, the H_1 resonance of methyl β-galactoside does not occur at the same chemical shift as the H_1' of deuterated methyl β-lactoside. Therefore, no direct TRNOEs to galactose protons should be produced on selective inversion at the chemical shift of the H_1' of methyl β-lactoside. All parameters for the control were the same as those used for the T_m = 0.2 s experiment in the deuterated methyl β-lactoside time course.

The 3.97 ppm peak is present in the control (Figure 5A). The additional peaks throughout the 3.6–3.9 ppm region and the β-Me peak most likely result from the partial inversion of the galactose H_1, and from spin diffusion from Rb to galactose. The uniform intensity across the galactose protons suggests that spin diffusion, rather than transfer from H_1, is likely to be the largest contributor to the sugar peaks here. Since galactose has no resonances at 3.97 ppm, we suggest this major peak to result from H_1–H_2 transfers on protein mannosides. These sugars have anomerics and H_2 protons in approximately the same positions as the H_1' anomeric and glucose H_{6a} protons (respectively) of methyl β-lactoside. The ricin B-chain has approximately 13 mannosides attached (Olsnes & Pihl, 1982). The mannoside H_1 protons would be inverted simultaneously with the deuterated methyl β-lactoside H_1'. Thus, the transfer from H_1' to H_{6a}, although expected to be small, cannot be quantitated accurately in the TRNOE experiment. The region showing H_4, H_5, and H_5' contacts fortunately remains relatively clear of intraprotein transfers in this control and encourages us to proceed with a more quantitative analysis.

As in the galactose case, we will have to deal with parameters for both free and bound forms of lactose. It is best to set the free-form parameters with data from an independent set of experiments, as done previously for methyl β-galactoside. We have therefore acquired a set of NOEs on a simple solution of deuterated methyl β-lactoside. A spectrum at T_m = 0.8 s is shown in Figure 6. The choice of longer T_m for illustration purposes is dictated by the less efficient cross relaxation for small molecules. Intensities at all mixing times show the expected patterns—strong NOEs to H_5' and H_4. Again, a transfer to the glucose H_5 is seen. However, the H_4 NOE appears smaller relative to the H_5' NOE in comparison to the ricin B-chain bound data. This observation was confirmed by integration using the curve-fitting routine. Thus, we expect some conformational differences between the free and bound states.

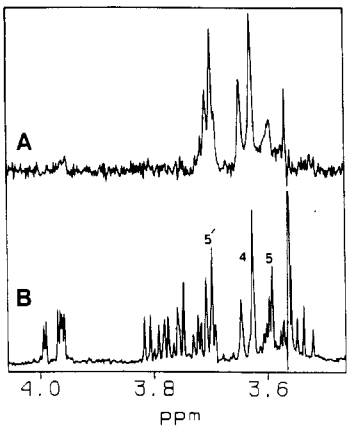

FIGURE 6: 490-MHz ^{1}H NMR spectra. (A) 1D SIR TRNOE difference spectrum of deuterated methyl β-lactoside (T_m = 0.8 s). (B) Deuterated methyl β-lactoside spectrum. Same processing as for Figure 5C.

Analysis will again proceed with a spectral simulation program. The β-Me protons of methyl β-lactoside are remote from the site of inversion and thus were not included. Furthermore, although we have eliminated some spin-diffusion pathways by deuteration (H_1' to H_3' or H_5' and then to H_4', for example), others remain (H_1' to H_4 and then to H_5, for example). The remaining pathways must therefore be included in the simulation. Starting points for the array of proton positions used to calculate σ_{ij} values were taken either from the crystal structure of β-lactose (Hirotsu & Shimada, 1974) or from a structure produced by minimizing the structure with the model-building program AMBER[2] and a parameter set developed in this laboratory (Scarsdale et al., 1988). Several additional modifications to the array had to be made to accommodate the partial deuteration of the molecule. Protons at positions where total deuteration occurred were removed as were protons at positions where more than 50% deuteration occurred. In the latter case, all positions were far from protons of interest and were not expected to make large relaxation contributions in any event. The H_{6a} proton, which is at a position found to remain 75% protonated, was set to 100%. The H_{6a}' and H_{6b}' protons are each at positions of about 50% remaining protonation. In the crystal structure, H_{6b}' is far from protons of interest and likey to produce small differences whether protonated or not. It was thus eliminated from the array. H_{6a}' is near H_5' and was thus treated more exactly by averaging simulation results from two structures, one in which H_{6a}' was present and one in which H_{6a}' was absent.

Simulations for the sugar free in solution were carried out by first attempting to fit the H_1', H_5', and H_4 experimental time course curves by use of the crystal structure geometry and by varying the correlation time (τ_c) and the external relaxation parameter. The H_5' and H_4 buildup curves of the free sugar time course could not simultaneously be fit with the crystal structure. This result was not surprising since the integral of the H_4 experimental NOE proves to be somewhat larger than the integral of the H_5' experimental NOE, but the H_5'–H_1' distance (2.31 Å) is shorter than the H_4–H_1' distance (2.42 Å) in the crystal structure.

The crystal structure was thus minimized with AMBER, resulting in a structure with an H_5'–H_1' distance of 2.48 Å and an H_4–H_1' distance of 2.26 Å. The resulting structure was

[2] AMBER 3.0 (U. C. Singh, P. K. Weiner, D. A. Case, J. Caldwell, and P. A. Kollman, 1986) is a program obtained through a licensing agreement with the Reagents of the University of California at San Francisco.

Table II: Structural Data

structure	torsion angles ϕ	torsion angles ψ	$r_{1'4}$ (Å) X-ray	$r_{1'4}$ (Å) simulation	$r_{1'4}$ (Å) 1D	$r_{1'4}$ (Å) 2D
crystal	+52	−8	2.42			
I (free)	+59	−7		2.36	2.31	2.39
II (bound)	+51	−5		2.22	2.19	2.11

therefore expected to lead to a simulated H_4 NOE greater than the simulated H_5' NOE. Simulation was carried out as before, with the AMBER-minimized structure. The size of the H_4 NOE relative to the H_5 NOE did increase, but judging from the simulations, the minimization appears to have reached a structure in which the H_4 is too close to the H_1' relative to the H_5' proton. Thus, the minimization/simulation cycle was repeated, this time with an H_1'–H_4 distance constraint, a different constraint being used each time until the experimental data could be fit. We will designate the resulting structure as structure I. The free sugar data on H_1', H_5', and H_4 could be fit well in a simulation using structure I, a τ_c of 1.2×10^{-10} s, and a ρ^* of 37%. H_5 and H_{6a} show small enhancements consistent with experiment, but because of possible strong coupling and internal motion effects not included in the simulations, fit to these curves was not included in the optimization.

The 37% ρ^* represents a lot of external relaxation, so several attempts were made to determine its origin. The sample was not purged with N_2, so it is possible that O_2 in the sample could cause a significant amount of external relaxation. However, an experiment on the same sample, only purged, gave results identical within experimental error. The possibility of the presence of paramagnetic ions was also explored by adding EDTA to the purged sample and repeating the time course with a small number of scans. The H_1 recovery curve again agrees well with those of the other experiments. Thus, the high ρ_f^* most likely results from leaving out some of the partially protonated positions in the simulation models or from the fact that solution conditions are not well modeled by a single rigid conformer.

By use of a single rigid structure model, the best-fit structure has an H_1'–H_4 distance of 2.36 Å, compared to the initial AMBER-minimized structure H_1'–H_4 distance of 2.26 Å. This distance (2.36 Å) is actually close to the crystal structure distance (2.42 Å), but in the AMBER structures the relaxed H_1'–H_5' distance was always 2.48 Å, as compared to the crystal structure distance of 2.31 Å. Thus, there is a significant departure in overall structure with a significant increase in the glycosidic torsion angle ϕ. A comparison of experimental data with simulation results is shown in Figure 7. Table II presents a summary of structural data.

In the ricin-bound methyl β-lactoside simulation, the parameters pertaining exclusively to the free state can again be taken from the fit described above. K_as for methyl β-lactoside bound to Rb are not known with great precision. However, for large K_as, most of the protein is bound, and simulations show little sensitivity to the actual value. A range of association constants from 10^3 to 5×10^4 M^{-1}, in agreement with data on related ligands (Houston & Dooley, 1982; Yamasaki et al., 1985; Hatakeyama et al., 1986), was tested. The closeness of fits of the experimental data in this K_a range varied only slightly. A K_a value of 2×10^4 M^{-1} was used in the remaining simulations. This value is a reasonable estimate on the basis of the fact that lactose ($K_a = 1.86 \times 10^4$ M^{-1}) binds more strongly to ricin than methyl α-galactoside and methyl β-galactoside and both methylated galactoses bind more strongly than the unmethylated species (Yamasaki et al., 1985). Furthermore, ligand/Rb association constants are on the same order as those of ligand/ricin systems.

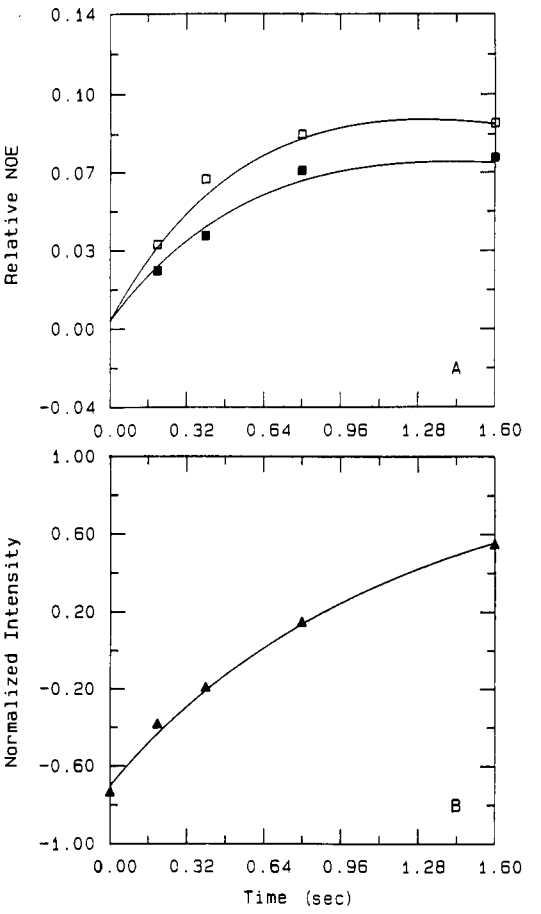

FIGURE 7: Experimental and simulated H_5' and H_4 curves for deuterated methyl β-lactoside alone in solution. Experimental results: (▲) H_1'; (■) H_5'; (□) H_4. Simulation results (—).

Initially, simulations were carried out with the bound structure having a conformation identical with the free structure (structure I). k_{-1} was varied from 40 to 10^5 s^{-1} as noted above. ρ_b^* and τ_{cb} were varied to give an optimum fit to the H_5' and H_1' curves at each k_{-1}. The results prove not to be greatly dependent on k_{-1} for these cases in which spin diffusion is limited and were constant above $k_{-1} = 10^2$ s^{-1}. H_5' and H_4 curves from the simulation with $k_{-1} = 50$ s^{-1} appear in Figure 8A. While the H_1' and H_5' data can be fit fairly well, it is clear from the graph in Figure 8A that a model with the same structure for the bound as for the free ligand does not allow fit of the H_4 curve (open squares). The experimental H_4 NOE is too large compared to the simulation, indicating that the bound-state H_4 is closer to the H_1' than the free-state H_4.

The AMBER minimization/simulation procedure was again carried out to bring the H_1' and H_4 closer together. Simulations were carried out for the various k_{-1} values, fitting H_1' and H_5'. Structure I was input as the free conformation, while a structure with a shorter H_1'–H_4 distance was input as the bound ligand. The best fit of the simulation to the experimental data occurred for a structure (structure II) where the H_1'–H_4 distance is 2.22 Å, with a ρ_b^* of 36% and τ_{cb} of 4.3×10^{-8} s. Results for $k_{-1} = 50$ s^{-1} appear in Figure 8B. The agreement between simulation and experiment for H_1', H_5', and H_4 is now much improved. Transfers from H_1' to H_5' and H_{6a} are small but slightly larger than those for structure I. The change at H_5' is qualitatively in agreement with experimental observation. But, again, because of inability to ac-

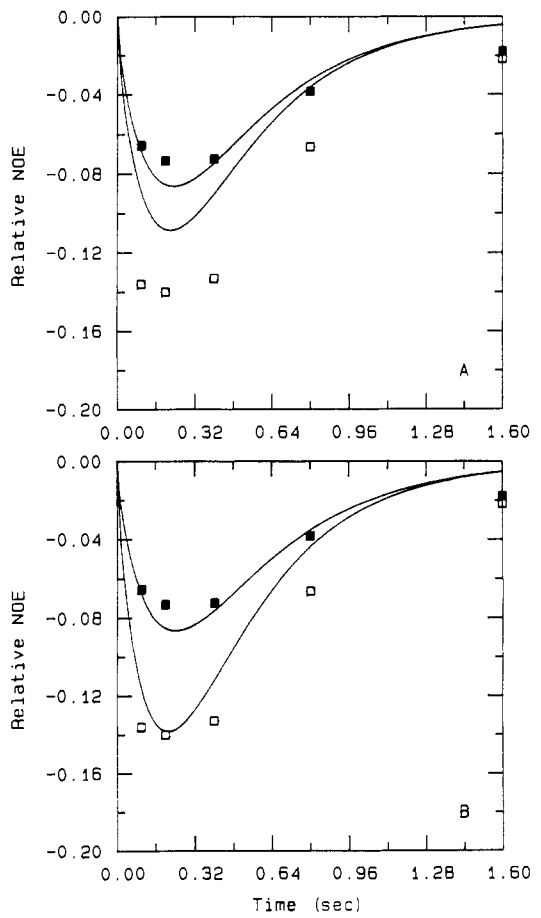

FIGURE 8: Experimental and simulated H_5' and H_4 curves for deuterated methyl β-lactoside in the presence of Rb. Sugar:protein = 6:1; k_{-1} = 50 s^{-1}. Experimental results; (■) H_5'; (□) H_4. Simulation results (—). (A) Simulation for structure I bound; (B) simulation for structure II bound.

curately quantitate the small NOE at H_{6a}, and because of imprecisions in modeling of these low-amplitude transfers, they were not explicitly included in our fitting procedure.

It is possible to get anomalously short distances in the above experiments because of transfers mediated by protein protons that are particularly tightly coupled to the sugar. If we assume that such protons are also tightly coupled to the rest of the protein protons, it is possible to test this assumption by perturbing the protein proton reservoir through continuous irradiation in a protein-rich region of the spectrum. We should then see selective transfers to the H_1' and H_4 resonances. The same deuterated methyl β-lactoside/Rb sample was thus irradiated for mixing times of 0.4 and 0.8 s in the methylene/methyl region of the Rb spectrum (approximately 1 ppm). This region was saturated, rather than inverted, to compensate for loss of magnetization via spin diffusion to other protein protons, and the difference spectrum was checked for specific protein to sugar transfers. The intraprotein transfer to a peak at 3.97 ppm was seen as with selective inversion at 4.43 ppm. This peak has been assigned to mannose H_2 protons on the glycosylated protein. Another specific intraprotein transfer just downfield of the H_5' chemical shift was also seen. Although the protein–protein diffusion obscures the H_5' chemical shift, diffusion to other resolved sugar protons was much less in magnitude than the protein-specific peaks and appeared constant at all sugar resonances. The fact that the diffusion to sugar resonances is small and uniformly distributed argues against a specific transfer pathway between the protein and the ligand H_1' and H_4 protons.

Torsion angles and H_1'–H_4 distance values are summarized in Table II. From the table, we see that free and bound H_1'–H_4 distances differ by 0.1 Å. We conclude that either a conformational change about the glycosidic bond which brings the H_1' and H_4 closer together occurs upon the binding of methyl lactoside to Rb or that Rb selects a conformation with close approach of H_1' and H_4 from among a distribution found in solution.

It is also interesting to examine our ability to extract geometrical information from initial rate data with the independent spin pair approximation (ISPA). Only the points before 0.4 s were used in this attempt. For calibration purposes, the H_1'–H_5' distance is assumed to be 2.48 Å, equal to that in all AMBER-minimized structures. H_1'–H_4 distances calculated on this basis from 1D and 2D data are included in the last two columns of Table II. Differences are of the order of 0.1 Å, with the ISPA generally yielding shorter distances. However, it is interesting to note that trends in comparing free to bound remain qualitatively the same. The success of the ISPA, even in this qualitative interpretation, is dependent on our removal of several diffusion pathways by deuteration and use of NOEs from the early linear region in the buildup curve.

Although the conformational conclusions remain the same for all k_{-1} values simulated, a simulation of data on fully protonated lactose was carried out. In this case, the simulation proves to be more rate sensitive due to more extensive spin-diffusion pathways. The H_3', H_3, H_4, and H_5 spectral region is not easily resolved so we treated this region as one peak. Simulations at various k_{-1} values were carried out with K_a = 2×10^4 M^{-1} and with the same τ_{cf}, τ_{cb}, ρ_f^*, ρ_b^*, and molecular geometries as used in the deuterated case. The results (not shown) indicate a k_{-1} on the order of 50 s^{-1}, a value somewhat lower than that in the galactose case.

Conclusions

The transferred NOE experiment thus proves to be an extremely effective means of exploring the conformation and exchange dynamics of saccharides bound to the ricin B-chain lectin. Straightforward analysis of data on fully protonated ligands using equations based on the independent spin pair approximation proves to be misleading. However, selective deuteration and/or a complete relaxation matrix analysis allows determination of a bound structure. Moreover, when the molecule is fully protonated, the extensive spin-diffusion pathways render magnetization transfer sensitive to exchange rates. By using these methods, we have estimated the dissociation rate constant for methyl β-lactoside to be on the order of 50 s^{-1} and that of methyl β-galactoside to be on the order of 300 s^{-1}. These rates are consistent with moderate binding constants of the two ligands and well within the range allowed by diffusion limitation of on-rates. The slightly higher k_{-1} value for galactose compared to lactose is consistent with its lower binding constant.

The lactose geometry changes on binding are small but significant. If the free sugar is thought of as existing in a single conformation, the lactose can be said to undergo a conformational change upon binding to Rb which involves rotation about the glycosidic bond, bringing the H_1' and H_4 protons closer together by approximately 0.1 Å. More likely, the geometry change represents the selection of one conformer from a range of conformers existing in solution. The precise geometry changes reported must correspond to some weighted average of geometries for the two sites found on the ricin B-chain. However, given the structural homology within the sites, the effects of averaging may not be large. Rationalization for changes in geometry can, in principle, be sought by docking

the ligand in the two binding sites when the protein coordinates become available.

ACKNOWLEDGMENTS

NMR processing, display, and plotting routines were written by Dennis Hare, and integration routines were written by J. N. Scarsdale and Paul-James Jones.

REFERENCES

Araki, T., & Funatsu, G. (1985) *FEBS Lett. 191*, 121.
Clore, G. M., & Gronenborn, A. M. (1982) *J. Magn. Reson. 48*, 402.
Fischer, E., & Fischer, H. (1910) *Ber. Dtsch. Chem. Ges. 43*, 2521.
Hatakeyama, T., Yamasaki, N., & Funatsu, G. (1986) *J. Biochem. 99*, 1049.
Hirotsu, K., & Shimada, A. (1974) *Bull. Chem. Soc. Jpn. 47*, 1872.
Houston, L. L., & Dooley, T. P. (1982) *J. Biol. Chem. 257*, 4147.
Jeener, J., Meier, B. H., Bachmann, P., & Ernst, R. R. (1979) *J. Chem. Phys. 71*, 4546.
Koch, H. J., & Stuart, R. S. (1978) *Carbohydr. Res. 67*, 341.
Kumar, A., Ernst, R. R., & Wüthrich, K. (1980) *Biochem. Biophys. Res. Commun. 95*, 1.
Montfort, W., Villafranca, J. E., Monzingo, A. F., Ernest, S. R., Katzin, B., Rutenber, E., Xuong, N. H., Hamlin, R., & Robertus, J. D. (1987) *J. Biol. Chem. 262*, 5398.
Olsnes, S., & Pihl, A. (1982) in *Molecular Aspects of Cellular Regulation* (Cohen, P., & Van Heyningen, S., Eds.) Vol. 2, pp 51–105, Elsevier Biomedical Press, Amsterdam.
Olsnes, S., Refsnes, K., Christensen, T. B., & Pihl, A. (1975) *Biochim. Biophys. Acta 405*, 1.
Paulsen, H., Hasenkamp, T., & Paal, M. (1985) *Carbohydr. Res. 144*, 45.
Rutenber, E., Ready, M., & Robertus, J. D. (1987) *Nature 326*, 624.
Scarsdale, J. N. (1989) Ph.D. Thesis, Yale University, New Haven, CT.
Scarsdale, J. N., Ram, P., & Prestegard, J. H. (1988) *J. Comput. Chem. 9*, 133.
Smith, F., & Van Cleve, J. W. (1952) *J. Am. Chem. Soc. 74*, 1912.
States, D. J., Haberkorn, R. A., & Ruben, D. J. (1982) *J. Magn. Reson. 48*, 286.
Sundler, R., & Wijkander, J. (1983) *Biochim. Biophys. Acta 730*, 391.
Takagi, S., & Jeffrey, G. A. (1978) *Acta Crystallogr. B34*, 2006.
Wider, G., Macura, S., Kumar, A., Ernst, R. R., & Wüthrich, K. (1984) *J. Magn. Reson. 56*, 207.
Yamasaki, N., Hatakeyama, T., & Funatsu, G. (1985) *J. Biochem. 98*, 1555.

O_2 and CO Reactions with Heme Proteins: Quantum Yields and Geminate Recombination on Picosecond Time Scales†

Mark R. Chance,*,‡ Scott H. Courtney,§ Mark D. Chavez,∥ Mark R. Ondrias,∥ and Joel M. Friedman§

Department of Chemistry, Georgetown University, 37th and O Street, N.W., Washington, D.C. 20057, AT&T Bell Laboratories, Murray Hill, New Jersey 07974, and Department of Chemistry, University of New Mexico, Albuquerque, New Mexico 87131

Received December 14, 1989; Revised Manuscript Received February 6, 1990

ABSTRACT: Picosecond time-resolved absorption spectroscopy and low-temperature studies have been undertaken in order to understand the nature of the intrinsic quantum yields and geminate recombination of carbon monoxide and oxygen to hemoglobin and myoglobin. We find that the photoproduct yields at 40 ps and long times (minutes) after photolysis at 8 K are similar; however, the yield of oxygen photoproducts is 0.4 ± 0.1 while the yield of carbon monoxide photoproducts is 1.0 ± 0.1 for both myoglobin and hemoglobin. Measurements in the Soret, near-infrared, and far-IR are used to quantitate the photoproduct yields. These results call into question previous cryogenic kinetic studies of O_2 recombination. Significant subnanosecond geminate recombination is observed in oxyhemoglobin down to 150 K, while below 100 K this geminate recombination disappears. The lower photoproduct yields for oxyheme protein complexes can be attributed to both subnanosecond and subpicosecond recombination events which are ligand and protein dynamics dependent.

Characterization of the photolytic reactions of ligand-bound hemoglobin and myoglobin is essential for understanding the kinetics and reactivity of heme reactions (Gibson, 1959; Antonini & Brunori, 1971; Gibson & Antonini, 1967). In general, the photoproduct yields are quite ligand-specific with the observed yield of photolysis products for NO and O_2 invariably lower than those for CO ligand. For example, the photoproduct yield for horse CO myoglobin on microsecond time scales is 1.0, while those for O_2 and NO ligands are 0.03 and 0.001, respectively (Antonini & Brunori, 1971). In addition, observed yields are affected by temperature, solution conditions, and protein structure (Gibson & Ainsworth, 1959; Saffran & Gibson, 1977; Brunori et al., 1973; Noble et al., 1967).

A major advance in the study of ligand–heme protein photodissociative events occurred with the discovery that geminate recombination on the 100-ns time scale contributes to the observed differences in longer time photoproduct yields (Duddell et al., 1979; Alpert et al., 1979; Friedman & Lyons,

† This work was supported in part by National Science Foundation Grant DMB-8604435.

* Address correspondence to this author.
‡ Georgetown University.
§ AT&T Bell Laboratories.
∥ University of New Mexico.

0006-2960/90/0429-5537$02.50/0